Structure−Property Relationships in the Crystals of the Smallest Amino Acid: An Incoherent Inelastic Neutron Scattering Study of the Glycine Polymorphs

Heloisa N. Bordallo,*,† Elena V. Boldyreva,‡,§ Alexandra Buchsteiner,† Michael Marek Koza,‖ and Sven Landsgesell†

Hahn-Meitner-Institut, Glienicker Strasse, 100 14109 Berlin, Germany, REC-008 Novosibirsk State University, ul. Pirogova 2, Novosibirsk 630090, Russia, Institute of Solid State Chemistry and Mechanochemistry, ul. Kutateladze 18, Novosibirsk 630128, Russia, and Institut Laue-Langevin, BP 156 - 38042 Grenoble, Cedex 9, France

Received: February 19, 2008; Revised Manuscript Received: April 3, 2008; In Final Form: April 4, 2008

Incoherent inelastic neutron scattering spectra for the three crystalline polymorphs (α- $P2_1/n$, β- $P2_1$, γ- $P3_1$) of glycine ($C_2H_5NO_2$) at temperatures between 5 and 300 K (using the time-of-flight (ToF) spectrometer NEAT at HMI) and at pressures from ambient up to 1 GPa (using the ToF spectrometer IN6 at the ILL) were measured. Significant differences in the band positions and their relative intensities in the density of states (DoS) were observed for the three polymorphs, which can be related to the different intermolecular interactions. The mean-squared displacement, $\langle u^2 \rangle(T)$, dependence reveals a change in dynamic properties at about the same temperature (150 K) for all the three forms, which can be related to the reorientation of the NH_3 group. Besides, a dynamic transition in β-glycine at about 230−250 K on cooling was also observed, supporting previously obtained adiabatic calorimetry data. This behavior is similar to that already observed in amorphous solids, on approaching the glass transition temperatures, as well as in biological systems. It suggests the onset of degrees of freedom most likely related to transitions between slightly different conformational orientations. The DoS obtained as a function of pressure has confirmed the stability of the α-form with respect to pressure and also depicted a sign of the previously reported reversible β−β′ glycine phase transition in between 0.6 and 0.8 GPa. Moreover, a remarkable kinetic effect in the pressure-induced phase transition in γ-glycine was revealed. After the sample was kept at 0.8 GPa for an hour in the neutron beam, an irreversible transition into a high-pressure form (different from the β′-form) occurred, although previously in X-Ray diffraction and Raman spectroscopy experiments a γ- to δ-glycine phase transition was observed above 3.5 GPa only.

Introduction

Glycine, $^+NH_3CH_2COO^-$, the smallest amino acid, is extensively studied as an individual molecule, in solutions and in the solid state (see ref 1 as an entry point). Crystalline glycine is interesting as an example of a very small organic molecule giving rise to several polymorphs when assembled in a three-dimensional periodic structure, depending on the subtle changes in the crystallization conditions, and as a biomimetic; the three polymorphs of glycine known at ambient conditions since the pioneering work by Bernal[2] (α-, β-, and γ-forms) mimic different types of layered (α- and β-forms) and helical (γ-form) structures of proteins (Figure 1). Crystalline amino acids are considered very useful for developing an understanding of the influence of crystal and molecular structure on lattice dynamics and can serve as model systems for protein dynamics.[3–5]

Motions in proteins cover time scales from femtoseconds (individual bond vibrations) to microseconds and longer (collective motions of bonded and nonbonded groups of atoms). Since all these motions are temperature-driven, the knowledge of the temperature effect on the protein flexibility is essential for understanding protein function. It is now generally accepted that not all the motions in proteins are sensitive to temperature in the same way. In this respect it is especially interesting to follow in details the motions of the same functional groups not in the biopolymers but in the simpler biomimetics, crystalline amino acids. Additionally, subtle volume changes that arise from changes in packing density due to the decrease in intermolecular distances in the H-bond network can be magnified by pressure. It should be noted that alterations in the spatial distribution of charges will contribute to the electrostatic interactions resulting in specific evolution of the structural conformation. In fact, since Bridgman's pioneering work[6] in 1914, showing that a pressure of 0.7 GPa is able to denature proteins of egg white in a similar but not identical way as temperature, pressure effects have been long puzzling to biochemists.

In all the three polymorphs of glycine, there are head-to-tail chains of zwitterions linked by NH···O hydrogen bonds. These chains are very robust and are preserved even during the polymorphous transformations. Therefore, although there are no covalent peptide bonds within the chains, they can be considered to mimic the peptide chains in biopolymers.[7] The three glycine polymorphs differ by the strength of the intermolecular hydrogen bonds that link together the head-to-tail chains of the zwitterions in the crystal. In the α-polymorph, space symmetry group $P2_1/n$, the chains are linked by hydrogen bonds in double antiparallel layers,[8] the interactions between these double layers being purely

* To whom correspondence should be addressed. E-mail:bordallo@hmi.de. Phone: +49 (0)30 8062 2924. Fax: +49 (0)30 8062 2781

† Hahn-Meitner-Institut.

‡ REC-008 Novosibirsk State University.

§ Institute of Solid State Chemistry and Mechanochemistry.

‖ Institut Laue-Langevin.

10.1021/jp8014723 CCC: $40.75
Published on Web 06/26/2008

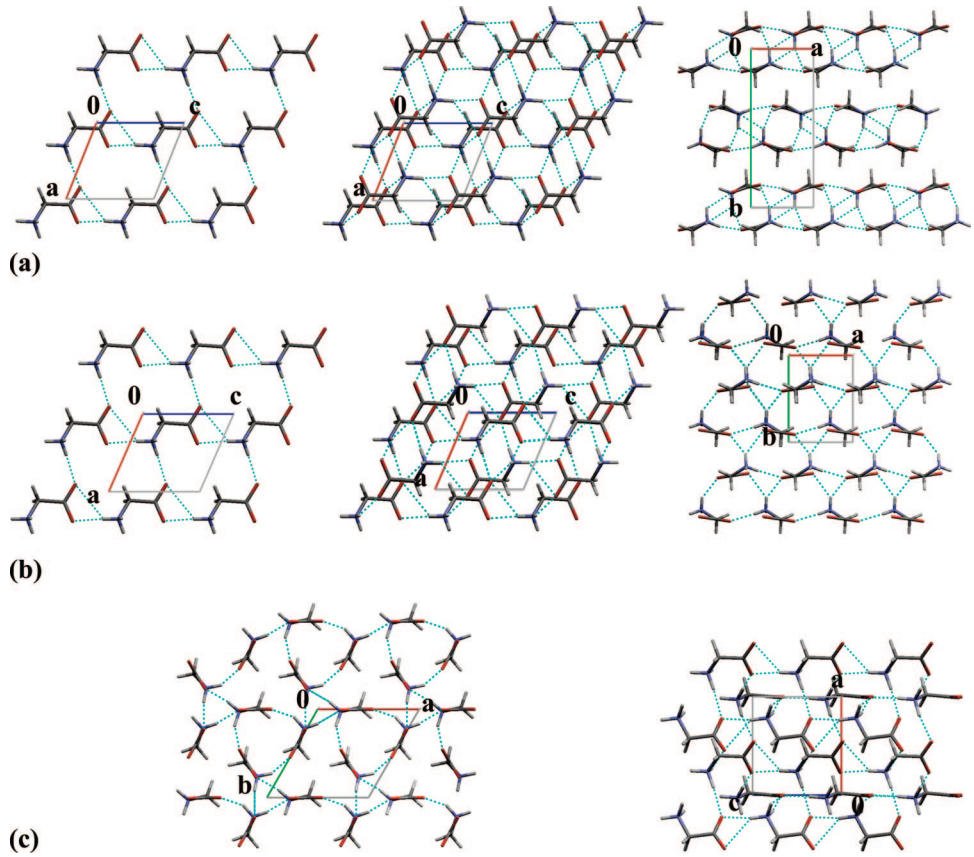

Figure 1. Fragments of the crystal structures of three polymorphs of glycine ($C_2H_5NO_2$): α-glycine (a), β-glycine (b), γ-glycine (c). ***a***, ***b***, and ***c*** indicate the crystallographic axes.

van der Waals. In the β-polymorph, space symmetry group $P2_1$, individual parallel layers are linked by H-bonds in a 3D network[9]. In the γ-polymorph, space symmetry group $P3_1$, chains of zwitterions form triple helixes linked with each other in a 3D network.[10]

The three crystalline forms show a striking difference in the response to variations in temperature and pressure. This holds for the absolute values of the bulk compressibility on cooling and, with increasing pressure, for the anisotropy of lattice strain,[11,12] and for the stability with respect to phase transitions.[13–24] The α-form is the easiest one to crystallize from an aqueous solution, and once formed, it remains stable with respect to variations in temperature[11,13–15,18] or pressure (at least up to 23 GPa)[19]. It converts into the γ-polymorph if kept in humid NH_3 vapor.[13,14] This high structural robustness is ascribed to the stability of the centro-symmetric double layers (an extension of the centro-symmetric dimers preserved in aqueous solution). The β-polymorph is metastable at all the temperature and pressure conditions and transforms spontaneously on storage, or on heating, either into the α- form (in the presence of water vapor), or into the γ-form (in the presence of humid NH_3).[13,14] In the dry environment, however, the β-form can be preserved for an indefinitely long time.[9,13,14,16,25,26] A second-order phase transition at about 250 K was observed in the β-form on cooling by adiabatic calorimetry,[14,16] and a reversible single crystal to single crystal phase transition into another layered polymorph was registered at about 0.76 GPa by Raman spectroscopy,[20] X-ray single crystal,[24] and high-resolution powder[27] diffraction (the β'-form, as named in ref 20, or the δ-form, as renamed in ref 24).

It was also observed that the multiple cycling of the temperature around the second-order phase transition point (~250 K) provokes a first-order β- to α-phase transition, presumably induced by lattice instability.[16] The γ-polymorph is thermodynamically the most stable form at ambient conditions.[9,13,28] It shows only a weak anomaly in heat capacity at 10 K,[13,15] and transforms into the α-form on heating or on storage in the presence of water vapor. With increasing pressure, a single crystal to powder irreversible phase transition was observed by X-ray diffraction[17,21,22,24] and Raman spectroscopy[23] in a wide pressure range starting from 3.5 GPa; on decompression, the high-pressure phase (the δ-phase, as named in ref 22, or the ϵ-phase, as renamed later in ref 24, which is a layered polytype of the α- and β-forms) transforms into one more layered polytype, namely, the ζ-form[23] at about 0.62 GPa.

Thus, glycine polymorphs provide an example of a strong dependence of the properties of a three-dimensional assembly of small molecules on its structure. The nature of this structure−property relation can be understood better if the dynamic properties of the crystal structures are also considered. Spectroscopic techniques can provide valuable information in this respect.

Vibrational spectra of an individual glycine molecule (neutral and as a zwitterion) as well as of the three polymorphs of glycine at ambient conditions, at variable temperatures, and with increasing pressure were repeatedly studied by computational and experimental techniques. However, phase purity of the samples is probably the main problem when comparing the properties of glycine polymorphs, since crystallization of several polymorphs is often concomitant and special care is required in order to get pure phases. In some publications, the polymorph of glycine is not defined at all, and the sample is qualified simply as "glycine". Additional problems are related to the fact that the IR-spectra of the glycine polymorphs are sensitive to the

sample preparation; maximum positions and relative intensities of the vibrational bands related to the NH_3^+ and COO^- groups differ quite noticeably for the samples compressed into the KBr pellets, or studied in Nujol, in Fluorolube or for the "free" nondiluted samples. Recently, a careful comparative study of the IR spectra of the three pure polymorphs of glycine registered in a wide temperature range (93−433 K) was published.[29] Since in ref 29 the spectra were recorded under identical conditions for nondiluted "free" well-characterized pure phases of all the three polymorphs, we shall refer for a comparison to these data when discussing the results of the present neutron scattering study. The same paper can be used as an entry point to the extensive literature on the vibrational spectra of glycine. Raman spectra were reported for the single crystal and powder samples of pure α-glycine on cooling from ambient temperature down to 83 K (in the limited spectral ranges 470−540 cm^{-1} and 3200−3050 cm^{-1}).[18] Variable-pressure Raman spectroscopy data were published for single crystals of β-glycine,[20] α-,[19] and γ- glycine[23] (spectral range 160−3300 cm^{-1}). Polarized Raman spectra for single-crystals of the α-[20] and the γ- glycine[31] were recorded only for ambient temperature.

The low-frequency vibrations of crystalline amino acids are of a special interest, since they contain information on the coupling between the internal motions of molecular fragments and the translational excitations, which can be related to the protein dynamics.[5] Librons (30−120 cm^{-1}), which are torsional oscillations of the amino acid or peptide chains, have long life times (10 ps $< T <$ 5 ns); at low temperature, the lifetime of these librons can even exceed 4 ns, and it decreases rapidly with increasing temperature, so that by 100 K the life times are in the 20 ps range.[5] The motions similar to the relaxation of excited torsional oscillations to lower frequency modes, which are observed in the crystalline amino acids at low temperatures, dominate the atomic mean square displacements in proteins at ambient temperature and have functional significance, e.g., facilitating migration of small ligands through biopolymers by structural fluctuations, opening the gateway to the ligand binding sites, and altering the ligand binding barrier.[5] The low-frequency range of vibrational spectra of glycine (presumably, in all the cases of the α-form, although not always specified explicitly) was studied by ps CARS[5], far-infrared,[32–36] Raman,[37,38] and, recently, by terahertz spectroscopy (the latter for α- and the γ-polymorphs at 300 K)[39] in all the cases, either at room temperature or at a single low temperature only.

Among other spectroscopic techniques, incoherent inelastic neutron scattering (IINS) has several advantages, especially in the low-frequency range, due to the strong incoherent scattering from protons. In fact, scattering by hydrogen is considerably stronger than by any other nucleus and thus dominates the signal if present; thus effects involving the dynamics of hydrogen atoms can definitely be observed.[40,41] Up until now, IINS spectra have been reported for several crystalline amino acids.[42–46] α-Glycine (C- and D-deuterated isotopomers) was studied by IINS at 20,[35,47] 100,[48] and 300 K.[49] In ref 50, the interaction between water and some amino acids (glycine, L-glutamine, L-threonine, L-cysteine, and L-serine) was studied. The spectra of dry samples and of wet frozen samples were measured at 10 K. The difference spectra (obtained by subtracting the spectrum of a wet frozen sample from that of the corresponding dry one) were similar to the spectrum of ice Ih for all the amino acids studied (glycine included), with the only exception of L-serine that presumably forms a hydrate on freezing. No IINS data for γ- and β-glycine have been ever reported.

As we have shown in a recent IINS study of the crystals of L- and DL-serine,[51] having spectra measured at a single point at low temperature, or even at two points (including the ambient-temperature measurement), is surely not enough to detect subtle dynamic transitions in a crystal. To the best of our knowledge, the measurements of the IINS spectra of a crystalline amino acid at multiple temperature points in a wide range were carried out only for L- and DL-serine[51] and L-alanine.[52] Neither are we aware of high-pressure measurements of the IINS spectra of a crystalline amino acid, although the neutron scattering data at variable pressures for other hydrogen-bonded crystals, like ammonium halides, for example,[53,54] were reported and proved to be helpful in elucidating the nature of the pressure-induced phase transitions.

Summing up the published literature on glycine, we can conclude that although glycine is a small molecule, it is a complex system that provides a challenge to study the interrelation between the intermolecular hydrogen bonding, intramolecular motions, static, and dynamic properties of the crystal structure, since its polymorphs have the highest concentration of hydrogen bonds per volume among all the crystalline amino acids and peptides.[5] This may explain, why despite the enormous number of publications devoted to the dynamic properties of glycine, many knowledge gaps still remain to be filled in.

One of the central problems remaining unsolved is the mobility of which groups is the driving force for the structural transitions (or instabilities), and how is it interrelated to the intermolecular hydrogen bonding and molecular packing in the crystal? In the present publication we have tried to approach this problem by comparing the IINS spectra of the three polymorphs of glycine at ambient conditions, at multiple points on cooling from the ambient temperature down to 5 K, and with increasing pressure up to 1.0 GPa in order to test if the data can assist in understanding the dynamics of the three different crystal structures and the origin of their very different stabilities with respect to variations in temperature and pressure.

Experimental Details

Glycine Samples. To facilitate the data comparison, essentially the same samples were used as previously for IR studies.[29] The three polymorphs (α-$P2_1/n$, β-$P2_1$, and γ-$P3_1$ ($P3_2$)) were prepared as described in refs 13, 14, and 55: the α-form crystallized from an aqueous solution at ambient conditions, the β-form precipitated from an aged acetic acid solution using acetone as antisolvent, and the γ-polymorph obtained by exposing the α-form to wet NH_3. The phase purity for the α- and γ-forms was checked by X-ray powder diffraction using a Bruker GADDS. The β-form, synthesized immediately before the experiments, was checked using a Bruker D8 Advance reflection mode X-Ray diffractometer. Special care was taken to keep the samples absolutely dry under all the experimental conditions.

Neutron Scattering Measurements. Neutrons may be scattered coherently or incoherently by the nuclei. With coherent scattering, the pair correlation of atoms can be studied, and thus one gets information on the structure of a system. On the other hand, incoherent scattering mixes the phases between scattering centers and only the self-correlation can be investigated. If the energy of a neutron remains unchanged when it interacts with a nucleus, the scattering is elastic. If a change in the kinetic energy of the neutron occurs, then the scattering is either quasi-elastic or inelastic. Molecular and lattice vibrations are more often studied through incoherent inelastic neutron scattering (IINS). As already mentioned in the Introduction, due to the

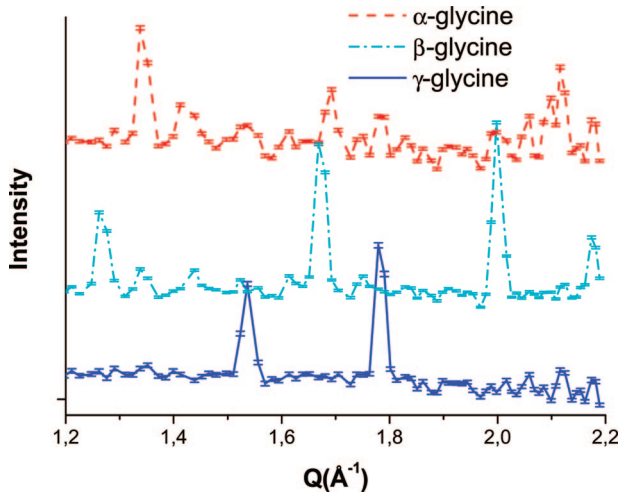

Figure 2. Time-of-flight diffraction patterns of α-glycine (red, dashed line), *β*-glycine (cyan, dotted-dashed line), *γ*-glycine (blue, full line) at 300 K.

exceptionally high incoherent cross-section of hydrogen compared to any other element, displacements involving hydrogen dominate in neutron spectroscopy. IINS in polycrystalline glycine polymorphs was measured using the time-of-fight (ToF) spectrometers NEAT[56] located at the Hahn-Meitner-Institut (HMI) and IN6 at the Insititut Laue-Langevin (ILL). Both spectrometers are designed for quasi-elastic and (incoherent) inelastic neutron scattering.

NEAT Measurements as a Function of Temperature. As each polymorph presents a unique network of the intermolecular hydrogen bonds (Figure 1), accordingly, distinctive lattice mode contributions are expected in the low frequency region. The evolution of the IINS was monitored using this spectrometer between 100 and 300 K, with an incident wavelength $\lambda = 5.1$ Å (elastic resolution, full width at half-maximum (fwhm) 98 μeV). Data were collected in 388 ^{3}He counters covering an angular range from 13.35 to 136.65 degrees. Slab geometry with glycine samples thickness of 0.4 mm (mass ranging from 0.7 to 1.8 g, calculated normal-beam transmission of about 0.9) were used to achieve high total scattered intensities. An orientation angle of 135° with respect to the incident neutron beam direction was used for all samples, including vanadium. By employing this orientation, the higher detectors have to be discarded. For the data analysis, after removing Bragg peaks, the spectra were transformed into the partial differential scattering cross-section and, finally, to the generalized density of vibrational states G(ω), following a classical approach.[57] In order to get an insight to the quasi-elastic (QE) signal, the spectra were averaged over the whole angular range covered by the spectrometer. This averaging procedure led to a better deconvolution of the QE components, even if the Q-dependence of the proton dynamics could not be analyzed. The spectra correction, normalization, grouping, and transformation to the energy transfer scale were performed using standard routines available at HMI. In addition to giving information on IINS response in the region of medium to very small E and Q, including QE (quasi-elastic) scattering, NEAT can also be used for diffraction experiments. Figure 2 shows the patterns at 300 K obtained for each polymorph. This is helpful to check the phase composition during the IINS experiments in situ.

IN6 Measurements as a Function of Pressure. The instrument IN6 provides a very high flux of cold neutrons, which is an essential requirement for the present study. The incident wavelength was chosen to be $\lambda = 4.14$ Å. As we address a broad range of energy transfers, the monochromatic focusing geometry was used. Therefore the elastic resolution amounts to 170 μeV full width at half-maximum with time focusing on the elastic line. Data were collected in 235 ^{3}He counters covering an angular range from 10 to 113°. The glycine powder was mounted inside of a clamped cell. The sample is contained in an alumina (Al_2O_3) cylinder (42 mm long, with inner diameter equal to 0.6 mm), then placed between two opposing cylindrical tungsten carbide pistons, and loaded to variable pressure in a press between 0.2 and 1.0 GPa. Finally, the cell is clamped using a locking nut. Hydrostaticity is ensured by immersing the sample in Fluorinert FC75, (C_8F_{18}).[58] As the measurements were done at room temperature, no cryostat was used, allowing for a further decrease of the background. Typical counting times varied between 3 and 10 h. The raw data were corrected for the contributions of the pressure cell, and after corrections for the energy dependence of the detector efficiency, the scattering law, $S(Q,\omega)$ and $G(\omega)$, were obtained.

Theoretical Background: Incoherent Inelastic Neutron Scattering

Measuring dynamic properties constitutes one of the most powerful ways of getting insight on experimental details about the strength of atomic interactions. In particular, incoherent inelastic neutron scattering provides a most suitable probe for studies of vibrational dynamics for given solids. This is because of several remarkable properties of neutrons. For instance, the neutron energy is comparable to the phonon energy and the wavelength associated with the neutron is of the same order as the interatomic distances in condensed matter. Another characteristic of this probe is that the neutron mass is of the same order as the mass of the scattering nuclei. The scattering is, therefore, sensitive to the structure of the system. In an incoherent inelastic neutron scattering experiment, the variation of scattering intensity with neutron energy and momentum transfer is observed.

Depending on the temperature and energy resolution (time) range, the measured scattering function ($S(Q,\omega)$), where Q is the magnitude of the scattering wave vector and ω is the energy transfer, will express different contributions. This function can be decomposed into three components: elastic, QE, and inelastic (IN). The elastic component originates from neutrons without change in energy, and the inelastic component is related to vibrational modes. QE scattering, which is a broadening of the elastic peak, describes the dynamical nature of the molecular motion, and in this particular study will be dominated by the incoherent cross section of the hydrogen. IN scattering is related to the vibrational levels of the molecule. Thus, to get hold of an overall view of the dynamics in glycine, we carefully inspected the evolution of the elastic incoherent scattering intensity (probed $S(Q,\omega=0)$) as a function of the temperature. To do so, using a ToF spectrometer, it is necessary to analyze the intensity in the elastic peak channel as a function of temperature. At low temperatures, the linear decrease of the normalized elastic scattering $[S(Q,0)(T)/S(Q,0)$ $(T \sim 0$ K)] on a logarithmic scale, is described by the Debye−Waller factor:[59]

$$S(Q,\omega\approx 0) = \exp(-\langle u(T)^2\rangle Q^2/3) \quad (1)$$

where $\langle u^2(T)\rangle$ is the mean square displacement of the atoms around their equilibrium positions. Due to the larger incoherent cross section of the hydrogen, the measured $\langle u^2\rangle$ corresponds in practice to the H atoms. Being trapped in harmonic potential wells at low temperatures, the protons will jump between

different wells, if sufficient thermal energy is given to them, thus inducing a change in slope of the observed $\langle u^2 \rangle$. This temperature dependence of the dynamical relaxation process is entirely due to the temperature dependence of the motional timescales[60].

Besides, to address the effect of the $^{+}NH_3-CH_2-CO_2^{-}$ zwitterions interaction in the hydrogen bond network of the glycine polymorphs as well as to check if differences are observed due to the crystal structure, the IN part of the spectra was carefully analyzed. In a neutron scattering experiment, neutrons that enter the sample with defined momentum (Q_i) and energy (E_i) are scattered by the atomic nuclei and leave the sample with changed momentum (Q_f) and energy (E_f). The momentum transfer (Q), $\hbar Q = \hbar k_i - \hbar k_f$, will carry information about spatial distance,[61] while the energy change $\hbar\omega = \hbar E_i - \hbar E_f$, provides information on the time scale of the motion (time t and the energy $\hbar\omega$ are inversely proportional). For the particular case of incoherent scattering, in the one-phonon approximation, we have[57,62]

$$S_{inc}(Q,\omega) \propto \sigma Q^2 e^{-Q^2\langle u^2\rangle/3}\frac{n(\omega)+1}{\omega}g(\omega) \qquad (2)$$

where σ is the neutron total scattering cross-section of each element that is independent of the chemical environment, $n(\omega)$ represents the Bose occupation factor, and $\langle u^2(T)\rangle$ is the mean square displacement of the atoms.

In fact, (eq 2) reveals that the intensity of a mode is independent of the electronic properties of the material and solely dependent on the nuclear scattering cross-section, the momentum transfer, and the vibrational amplitudes of the atoms involved in that particular mode. The simplicity of the neutron−nucleus interaction has two important consequences, namely, first, that there are no selection rules in contrast to Raman and infrared spectroscopy and that all modes can in principle be observed. Second, it is straightforward by using DFT calculations to generate the dynamical matrix, which on diagonalization gives both the frequencies (from the eigenvalues) and the intensities (from the eigenvectors). For inelastic scattering spectra, this information is sufficient to calculate the whole spectral profile of a molecule or molecular group.

Different Dynamical Regimes in Glycine Polymorphs Supported by Elastic Measurements

Different kinds of contributions to molecular motions are essentially not coupled, because of their respective timescales and amplitudes. Vibrational motions of a molecule occur on the $10^{-13}-10^{-14}$ s timescale and may be considered as independent from rotations which are much slower ($10^{-9}-10^{-12}$ s). The energy resolution of any spectrometer is finite, and its fwhm determines the slowest observable movements. In the configuration used here, the longest limit for dynamical phenomena is a few ps. Furthermore, by considering the edge of the experimental energy spectrum, it is equally possible to obtain the purely inelastic spectrum for low energy vibrational modes ($1 < E < 100$ meV)[63].

Results obtained from the "window-measurement", where only the elastically scattered intensity is probed, on α-glycine, β-glycine, and γ-glycine are presented in Figure 3. Although NEAT accesses a rather limited range of momentum transfer, Q ($Q = 4\pi\sin\theta/\lambda$, where 2θ is the scattering angle), i.e., from about 0.25 to 2.11 Å^{-1}, some information can be obtained by analyzing the Q dependence of the elastic scattering intensities ($S(Q,0)$). $S(Q,0)$ for some selected temperatures are shown in Figure 3a. It can be seen that the ln $S(Q,0)$ curves are linear versus Q^2 at the lower temperatures, whereas a nonlinear behavior is observed for the higher temperatures. This behavior is reminiscent[60] of the one observed in amorphous solids on approaching the glass transition temperature as well as to the onset of torsional jumps between states of different energies. Evaluating $[S(Q,0)(T)/S(Q,0)\ (T \sim 0\ K)]$, $\langle u^2 \rangle$ was estimated as shown in Figure 3b. Data have been normalized to give $\langle u^2(5\ K)\rangle = 0$. Assuming that the Debye model is applicable (what is proven by adiabatic calorimetry to be the case for the α- and the β-glycine in all the temperature range[15,16] and for the γ-polymorph, with the exception at very low temperatures[15]), the data given in Figure 3b were fitted in terms of the following expression.[61]

$$\langle u^2 \rangle = \frac{3\hbar^2 T}{m k_B \theta_D^2}\left[\Phi\left(\frac{\theta_D}{T}\right) + \frac{1}{4}\left(\frac{\theta_D}{T}\right)\right] \qquad (3)$$

Where $\hbar$ is the reduced Planck constant, T is the temperature, m represents the mass of the scatters, k_B is the Boltzmann constant, and θ_D is the Debye temperature. $\Phi(x)$ is the Debye integral defined by

$$\Phi(x) = \frac{1}{4}\int_0^x \frac{y}{e^y - 1}\,dy \qquad (4)$$

The integrand in eq (4) can be expanded in a power series as:

$$\Phi(x) = 1 - \frac{x}{4} + \frac{x^2}{36} + ... \qquad (5)$$

At high temperatures, $T \ll \theta_D$ or $x < 1$,

$$\Phi(x) = 1 - \frac{x}{4} \qquad (6)$$

implying that the Debye−Waller factor will be linear with temperature.

$$\langle u^2 \rangle = \frac{3\hbar^2 T}{m k_B \theta_D^2} \qquad (7)$$

For the low temperatures, where $T \ll \theta_D$, the exponential in the denominator of eq 4 becomes very large before reaching the limit, zero point motion is dominant, and $\Phi(x) = 0$. Consequently, the Debye−Waller factor becomes temperature independent:

$$\langle u^2 \rangle = \frac{3\hbar^2}{4 m k_B \theta_D^2} \qquad (8)$$

Within the statistical accuracy of our data and the measured timescale, the mean square displacements relative to all samples obey the harmonic model up to 150 K whereas nonharmonic contributions (polymorph-specific motions) are evident at higher temperature.

Since glycine contains no methyl, or any other side groups, the change in the dynamic behavior of the glycine polymorphs at about 150 K can be supposed to be related to the freezing of the reorientational motions of NH_3 groups below this point.[52,64–68] The correlation time for such hopping is a thermally activated process related to the activation energy by an Arrhenius relation. Given that in a number of systems the potential barrier height obtained from neutron experiments compares favorably with the activation energies derived from NMR experiments and from inelastic neutron scattering results, [69–74] to analyze our data, we take into consideration previous proton NMR results. For example, continuous-wave NMR studies of the proton spectra

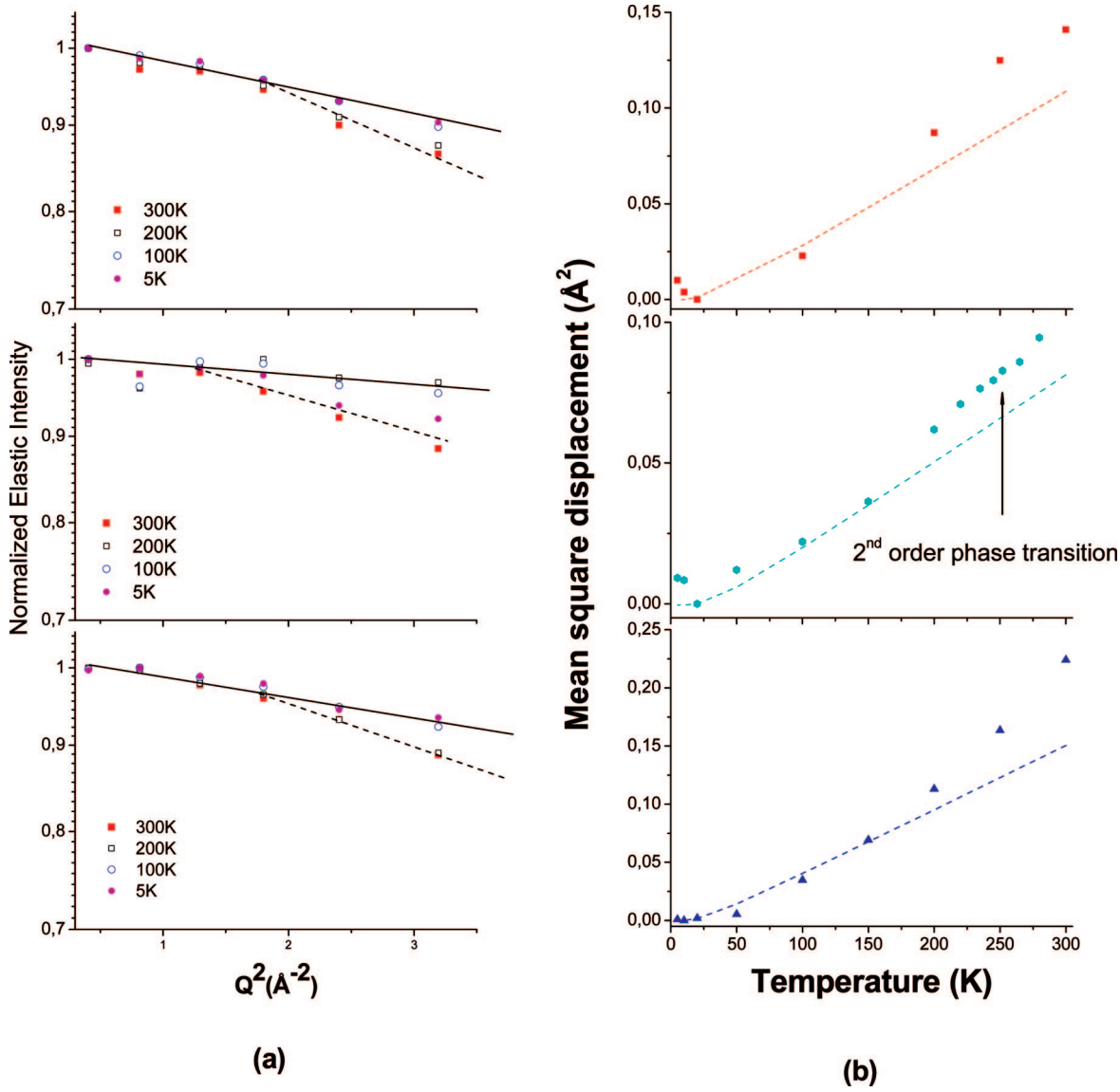

Figure 3. (a) Elastic scattering intensity vs Q^2 for α-glycine (top), and β-glycine (middle) and γ-glycine (bottom) at some selected temperatures. The lines are guides to the eye. The dotted line represents the deviation from linearity, i.e., from harmonicity. (b) $\langle u^2 \rangle$ was calculated by evaluating the Q dependence of $S(Q,0)(T)/S(Q,0)$ ($T \sim 20$ K) for α-glycine (top), β-glycine (middle), and γ-glycine (bottom). The dashed lines are the mean squared displacements calculated from elastic neutron scattering measurements (resolution 100 μeV), as described in the text.

of α-glycine exhibit spectral narrowing above 150 K caused by rapid reorientation of the $-NH_3$ group.[75] A single minimum of the relaxation time, T_1, with temperature is observed. Similar behavior (changes in the dynamics at a particular temperature, ranging for different amino acids between 150 and 400 K) was reported for aspartic acid, cystine, histidine, serine, tryptophan, and tyrosine,[66] when the source of relaxation is provided by reorientation of the $-NH_3$ group in the zwitterion form of the molecules and has been observed also in triglycine sulfate at about 150 K.[76] In L-alanine, large amplitude reorientations of the NH_3 moieties[77] are thermally activated around 220 K. According to the NMR data,[64,66,78,79] the activation energies of NH_3^+ group reorientation in the crystals of amino acids range from 28 to 40 kJ/mol. This suggests, that together with the intramolecular forces (which determine the staggered positions for the NH_3^+ groups as preferable), the barriers are to a large extent intermolecular in origin and dependent on details of the packing, hydrogen bonding, and electrostatic interactions.[66] For the polymorphs of glycine, the activation barrier for the reorientation of the NH_3 group is the lowest in the α-polymorph (23 kJ/mol)[79] as compared to the γ-polymorph of glycine (29−33 kJ/mol)[66,78,79] or to the β-glycine (44 kJ/mol)[80]. In the case of the α- and γ-polymorphs, the activation barriers for the NH_3 reorientation motions are very similar and such a transition can be directly related to the change in the slope of the $\langle u^2 \rangle(T)$ curves in the IINS experiments observed between 140 and 160 K. For the β-polymorph the activation barrier is noticeably higher, but the dynamic transition in IINS-experiments is observed at approximately the same temperature, as in the α- and the γ-polymorphs. One can suppose that the temperature dependence of the second moment of the NMR spectra of β-glycine contains two components, only one of which is related to the onset of the NH_3 reorientation motions. In such a case, the obtained activation energy would also contain a contribution of the proton displacement that would explain the weakening of the N−H···O bonds on cooling (unique for the β-polymorph, as compared to the α- and γ-forms), which was observed in IR-spectroscopy experiments.[29]

In contrast to other polymorphs of glycine, for the sample of β-glycine, another $\langle u^2 \rangle(T)$ line break was observed around 230−250 K. This break must correspond to a second-order phase transition detected previously by adiabatic calorimetry measure-

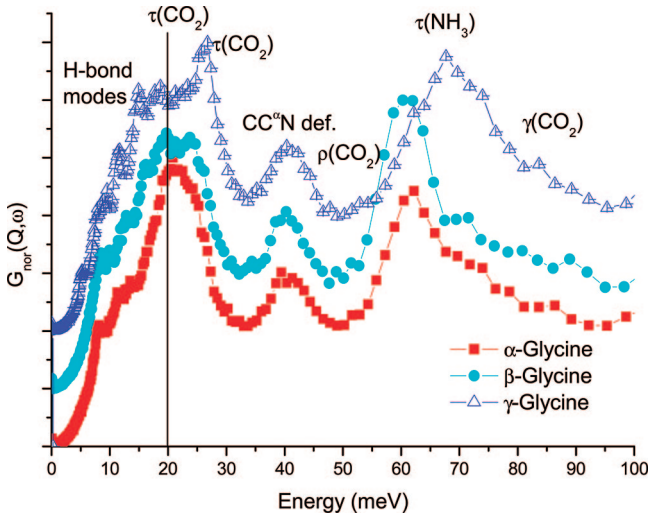

Figure 4. Density of states of the hydrogen atoms for (a) α-glycine (□), β-glycine (•), and (c) γ-glycine (△) at 300 K. The modes are assigned based on ref 29. The curves are displaced in the y-axis for clarity. The low frequency features (delimited by the vertical line at 20 meV) indicate the intermolecular vibrational modes region.

ments.[16] A comparative IINS study of the C- and N-deuterated α-, β-, and γ- glycine isotopomers would be very informative to understand the nature of motions involved in this phase transition in β-glycine as well as in the dynamic transition in all the three polymorphs at about 150 K. However, such a study is a real challenge, since deuteration may effect both the crystalization of the polymorphs and the phase transitions in the solid state (see as examples refs 77 and 81).

Dynamics and Packing of Molecules in Glycine Polymorphs

(a) Temperature Effects. The GDOS for glycine polymorphs calculated from NEAT data at 300 K is reported in Figure 4. The energy resolution in direct geometry is intrinsically better than in inverse geometry; however, direct geometry instruments are kinematically limited in energy transfer. Therefore the IINS spectrum is dominated by anti-Stokes scattering, i.e., it appears in the neutron energy gain side of the QE response, and will obey the Bose−Einstein statistics.[82] According to X-ray data,[8–11] α-glycine crystallizes in the $P2_1/n$ space group with $Z = 4$, β-glycine crystallizes in the $P2_1$ space group with $Z = 2$, and γ-glycine crystallizes in the $P3_1$ space group with $Z = 3$. Thus based on the factor group analysis method,[83] we find for the molecular vibrations a total of 120, 60, and 90 optical modes, respectively, of which 21 are lattice vibrations. The intensity profiles are quite different for the three polymorphs; similarly to other systems,[84] the higher molecular mobility in the γ-form can be related to the observation of the lowest vibration mode of all polymorphs. The assignment of lines in the IINS spectra of glycine in terms of torsion (τ), deformation (def), rocking (ρ), and wagging (γ) (based on the experimental data and theoretical calculations[29–31,36,37,85,86]) is indicated in Figure 4. The difference in the frequencies of each solid phase can be ascribed to variations of the intermolecular hydrogen bonding interaction in each crystal structure, which induce changes in the average force field. Lattice modes as well as skeletal contributions are expected below 20 meV. The $\tau(CO_2)$ dominates the region 20−30 meV, and the strong mode observed at about 40 meV can be interpreted as the skeletal deformation. The sharp IINS peak (at about 64 meV for α- and β-polymorphs and about 70 meV for γ-glycine) that cannot be seen in either Raman, or infrared data, is assigned to the NH_3^+ torsional mode. Since all the three available protons are used in forming N−H···O hydrogen bonds, the NH_3 torsional mode appears broad due to anharmonicity. Besides, due to the unequal strength of the three N−H···O bonds in glycine, the anharmonicity is greater as compared with alanine.[87] Another reason for the broadening is that carboxyl wagging and rocking motions are observed in the same region.[88] The decrease in the frequency of the NH_3^+ torsional mode ($\tau_\alpha \sim \tau_\beta < \tau_\gamma$) can be correlated with the increase in the hydrogen bond length.[11]

As shown in Figure 5, in the frequency region above 20 meV, most of the observed peaks are almost unchanged with temperature, except for the frequencies of two specific modes, $\tau(CO_2)$ and $\tau(NH_3)$, which in α- and γ-glycine harden with decreasing temperature, in agreement with the shortening of the intermolecular hydrogen bonds on cooling[11]. The small redistribution of the intensity under $g(\omega)$ is quite similar to the one observed in other soft systems; therefore, we can suppose that in α- and γ-glycine the NH_3 group dynamics includes a combination of torsional librations with rapid jumps between equivalent torsional positions, as was observed in alanine[52] and in acetanilide.[89] The redistribution of intensities is much more pronounced in the case of β-glycine between 300 and 245 K; below 200 K, the profile of the $\tau(NH_3)$ remains unchanged.

(b) Pressure Effects. *α-Glycine.* Figure 6 shows the neutron scattering spectra of the α-polymorph measured at various hydrostatic pressures up to 1.0 GPa. No significant shifts were observed either for the lattice modes or for the external modes. This result is in an agreement with the known fact that the α-polymorph is stable up to 23 GPa[19] and the structure is just compressed anisotropically, which results in changes in the N−H···O hydrogen bond interactions within a layer and a shortening in the distances between the double layers, as evidenced by X-ray diffraction.[12,24]

β-Glycine. A reversible single-crystal to single-crystal phase transition in β-glycine has been observed at 0.76 GPa using optical microscopy with polarized light, Raman spectroscopy,[20] X-ray single-crystal,[24] and high-resolution powder[27] X-ray diffraction. In the course of the phase transition, each of the individual molecular layers just splits into two sublayers due to a slight reorientation of every second molecule in the layer but the general molecular packing and, to a large extent, the three-dimensional hydrogen-bond network are preserved.[24,27] This transformation manifests itself clearly in the IINS. In Figure 7a, one can see marked softening of the lattice modes in β-glycine in a low-frequency range below 35 meV at the transition point. The significant intensity in neutron scattering spectra of this mode points toward a possible strong coupling of the C−C−N bond with NH_3 modes.

The spectra shown in Figure 7a correspond to the measurements on the freshly crystallized sample, which was compressed extremely slowly in an excess of Fluorinert, when filling in the sample holder. In contrast, when the same freshly crystallized sample was loaded into the sample holder quickly, with a uniaxial pressure of 1.0 GPa, an irreversible transformation of the β- into the α-polymorph was observed (Figure 7b). In this respect, it may be worthy noting that grinding of β-glycine is known to result in an irreversible β- to α-polymorph transformation,[13,14] whereas hydrostatic compression of the β-glycine gives the structurally closely related β'-polymorph at 0.76 GPa, which is then preserved at least up to 6.0 GPa[20,27] and the β-polymorph is restored on decompression.

γ-Glycine. The spectra of γ-glycine taken between ambient pressure and 0.6 GPa showed no significant changes, and neither

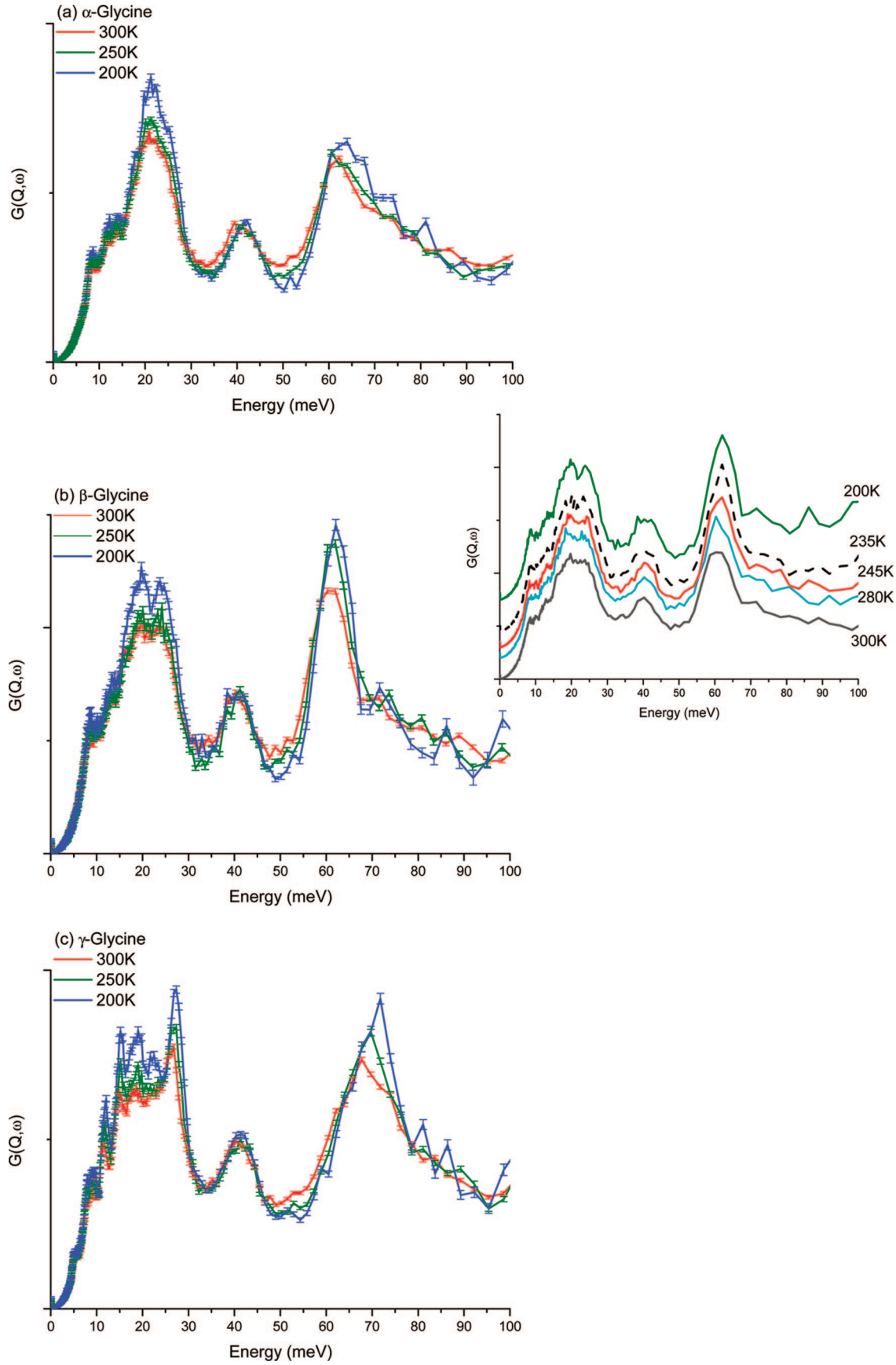

Figure 5. Density of states of the lattice phonons for (a) α-glycine, (b) β-glycine, and (c) γ-glycine as a function of temperature. The curves are corrected for the Bose temperature factor. The variation of both intensity and position of the $\tau(NH_3^+)$ for β-glycine as a function of temperature is also shown (b, insert). Note that below 235 K (i.e., below the phase transition) no further changes were observed.

did the spectrum obtained for the sample at 0.8 GPa change. However, after the sample was kept at this pressure for about an hour, the spectrum looked astonishingly different from those obtained at the same pressure before (Figure 8a). A washing

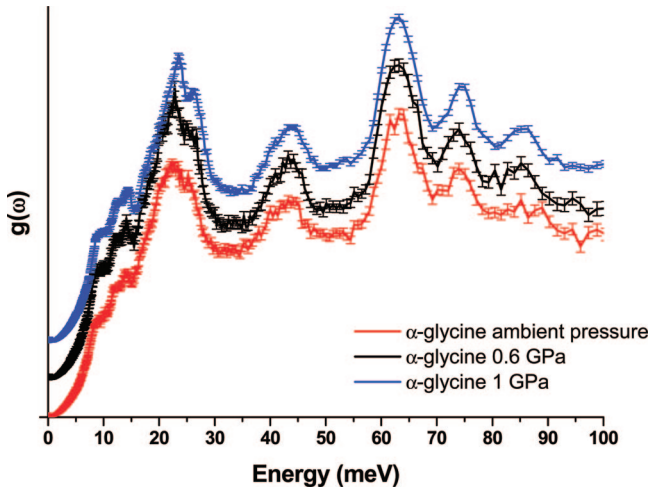

Figure 6. Density of states of the lattice phonons for α-glycine at 300 K as a function of pressure. The curves are displaced in the *y* axis for clarity. No significant changes in the IINS spectra or in the X-ray pattern indicate that no phase transitions occur between 0.2 and 1.0 GPa in α-glycine.

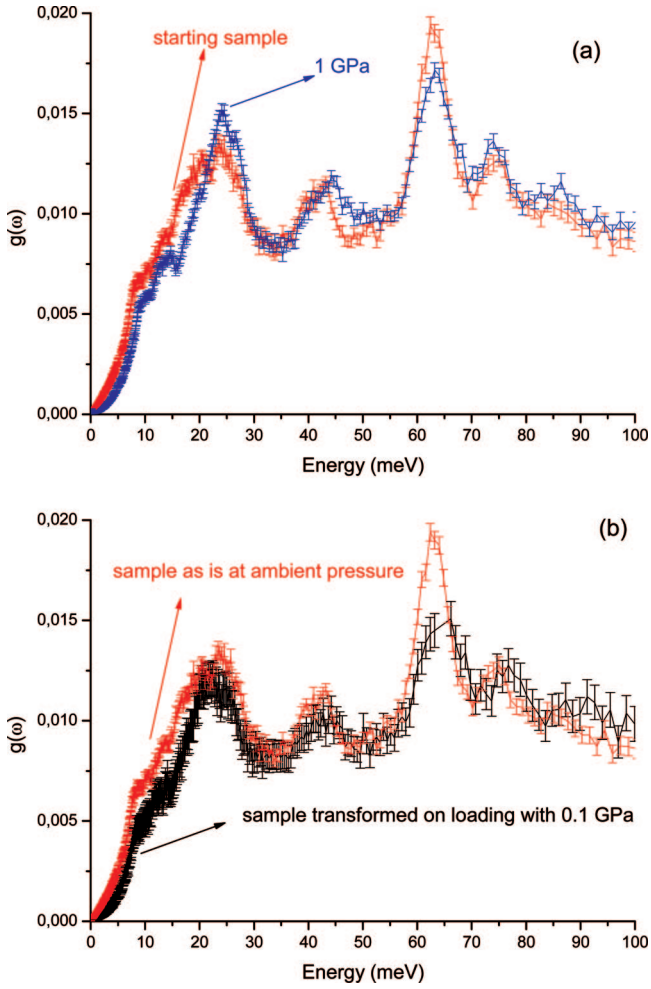

Figure 7. Density of states of the lattice phonons for β-glycine at 300 K as a function of pressure. (a) The previously reported phase transition is observed also in the IINS spectra between 0.6 and 0.8 GPa. (b) A transformation into the α-polymorph was observed after the sample was loaded into the pressure cell under nonhydrostatic conditions raising pressure quickly to 0.1 GPa.

out of the lattice mode located near 15 meV and of the mode associated to the $\tau(CO_2)$ near 25 meV plus a shift of the band

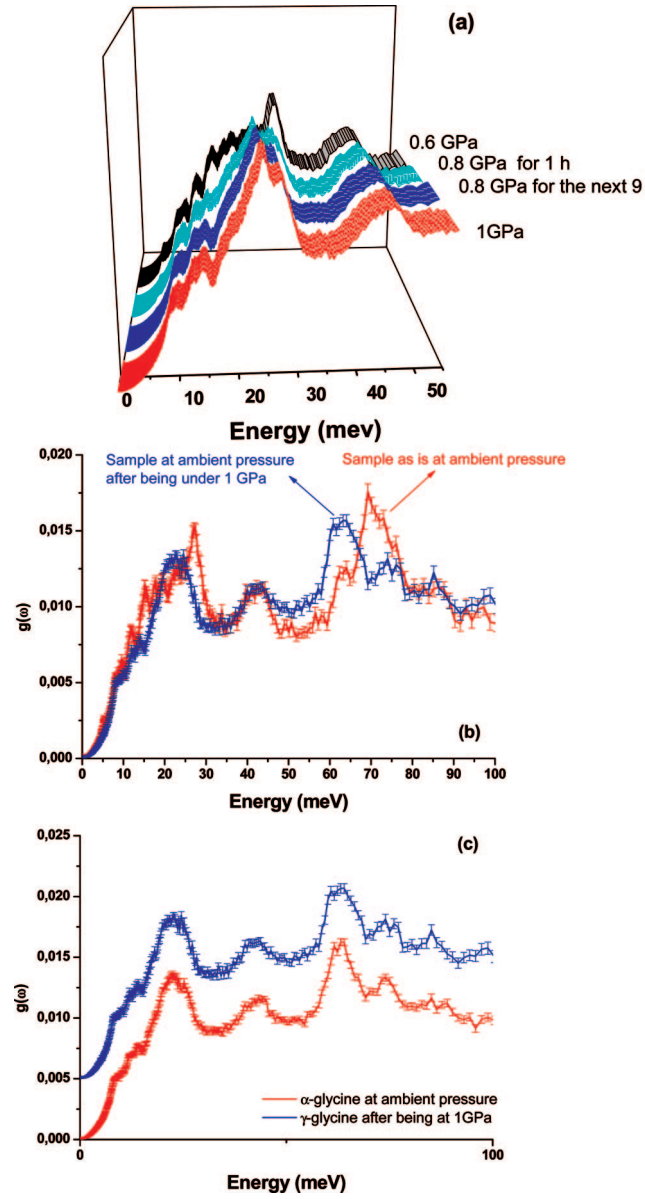

Figure 8. Density of states of the lattice phonons for γ-glycine at 300 K as a function of pressure. (a) A phase transition was observed after the sample was kept at 0.8 GPa in the neutron beam for more than 1 h. For clarity, only the spectra between 0 and 50 meV are shown. (b) Comparison of $g(\omega)$ measured at ambient pressure and after release of the applied 1.0 GPa pressure indicating that the phase transformation was irreversible. (c) Comparison of $g(\omega)$ measured at ambient pressure for α-glycine and for γ-glycine after release of the applied 1.0 GPa. Note that the decompressed γ-glycine sample is a layered polytype similar to α, β, δ and ζ polymorphs.

assigned to the $\tau(NH_3)$ near 70 meV toward higher energy were clearly visible. The spectrum obtained after decompression was very different from the one taken for the γ-form at atmospheric pressure and was similar, but not identical, to that measured for the α-form (Figure 8b,c). These results support the X-ray diffraction[17,22] and the Raman spectroscopy[23] data, that the pressure induced γ- to δ-phase transition involves a big change in the NH_3^+ moieties, as the triple helices formed by the head to tail chains of the zwitterions are substituted for layers. Moreover, this result suggests that a long-term storage of the powder sample of γ-glycine in Fluorinert at pressure as low as 0.8 GPa in the low-energy neutron beam has induced the same irreversible polymorphic transformation, as was observed previously in single crystals and powder samples of γ-glycine in the

methanol−ethanol mixture in a wide pressure range from about 3 to about 8 GPa (i.e., at pressures much higher than 0.8 GPa), when these samples were compressed quickly enough.[17,21–24] From the IINS data, we can presume that the decompressed sample must be either a δ- or ζ-form or a layered polytype similar to α, β, δ, and ζ polymorphs, but its structure still has to be determined. After the cell was opened and stored in air for some time, the sample converted into the α-polymorph of glycine.

Conclusion

Variations in temperature and pressure can be used as valuable tools for basic biophysical and biochemical studies as well as for applied research, for instance, in food and pharmaceutical technology. In biochemical processes, applied pressure can inhibit bacterial growth, affect virus vitality, and control the activity of enzymatic reactions, and the reasons of these phenomena are to be sought in the effects related to the dynamics of selected functional groups, distortion of hydrogen bonds, and the rearrangement of the secondary structure of biopolymers, an analogue of phase transitions in crystals. This is why detailed studies of pressure- and temperature-induced changes in the crystals of biomimetics like the polymorphs of glycine described in the present contribution are of general importance. Pressure and temperature variations allow probing the structure−dynamics−function relationship of proteins and molecular solids. These phenomena are accompanied by a variation of proton mobility, which can be readily studied using neutron scattering techniques; due to the large neutron−proton cross section, the neutron scattering signal measured is essentially due to the hydrogen atoms. Whereas variable-temperature studies are rather common, neutron investigations at high pressure is quite a recent field, and many difficulties can still be encountered during the experiment. For instance, the limits of the pressure range that also regulate the amount of sample that can be used require instruments with low background and high intensity plus allocation of a considerable beam time.

In the present contribution we have described the results obtained for biomimetic crystals showing a large number of phase transitions (that occur on cooling and with variations in hydrostatic pressure). An additional advantage of the choice of this system was that this small amino acid is a very strong incoherent scatter. By means of IINS, we were able to demonstrate that unique networks of the intermolecular hydrogen bonds in the glycine polymorphs indeed lead to distinctive lattice mode contributions in the low frequency region. The study has proven that IINS spectra can be used to follow the dynamic transitions in such systems on cooling and on compression.

As a result of the large number of modes, the strong incoherent scattering from protons, the powder average by the samples, and the relatively high Q numbers at the anti-Stokes side, the resolution of the IINS spectra appears to be limited, i.e., not all predicted modes were clearly identified. Although based on the mode determination approach, one expects to observe the same number of lattice vibrations ($3N - 3$, where N is the number of atoms) for all polymorphs; a much more disentangled spectrum is observed for γ-glycine, the crystal structure of which is significantly different from those of the α- and β-polymorphs. The volume per molecule is the largest in the β-polymorph and the smallest in the α-form, with the γ-form occupying an intermediate position in this series[11]. Conclusions based on comparing the values of the bulk density can be misleading, as our recent study of the crystals of L- and DL-serine has shown; the molecular mobility in a denser structure of L-serine with a three-dimensional hydrogen-bond network is higher than that in a less dense structure of DL-serine, in which molecules form double hydrogen-bonded layers because of the local molecular environment effects.[51] In the case of glycine, the structure of the γ-polymorph built of triple helices further linked in a three-dimensional hydrogen-bonded network seems to liberate internal motions not accessible to the layered α- and β-forms, similarly to the effect observed in the two crystal forms of lysozyme.[90] Figure 9, presenting the space-fill models for the layered (α- and β-glycine) and the helical (γ-glycine) structures, may provide some support for this assumption. The changes in the IR-spectra of the three glycine polymorphs on cooling[29] agree with the IINS data; many of the vibrational frequencies for the γ-polymorph are lower as compared to the α- and the β-forms, and their shifts on cooling are larger. At the same time, interestingly enough, despite this higher molecular mobility, both the relative volume changes and the linear strain in the directions of principal axes of strain ellipsoid on cooling and with increasing pressure are smaller in the γ-polymorph of glycine than in the two other forms.[11,12]

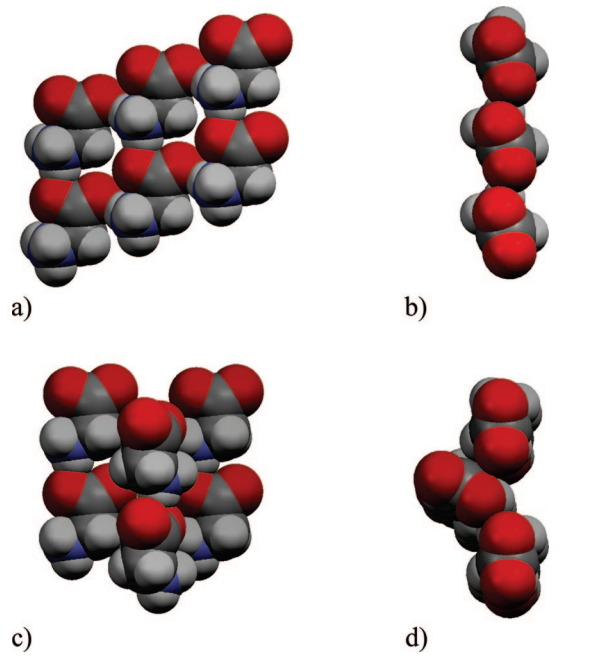

Figure 9. The space-fill models for the structural fragments of the α-, β- (above), and γ- (below) polymorphs of glycine in two orientations, illustrating a possibility of extra internal motions liberated in the γ-form and not accessible in the α- and β-forms.

The data on the low energy vibrations can be directly related to the mechanisms of the transformations between the forms and of more subtle dynamic transitions within the same polymorph as well as to the differences in the heat capacity of several polymorphs. It is possible to presume, for example, that the lowest frequency mode observed in γ-glycine at 5 meV can be associated to the small low-temperature anomaly of the specific heat capacity.[15] The temperature dependence of the Debye−Waller factors reveals that the polymorphs of glycine are nonharmonic solids. In the framework of the Debye−Waller model and within the experimental accuracy, γ-glycine shows a higher Debye temperature, confirming that its hydrogen bonds form a more rigid environment (compare with a biological system described in ref 91).

An important feature of the biopolymers (which is important for their functions) is that different fragments are activated at different temperature ranges and at different timescales. There-

fore, different experimental techniques may give data leading to seemingly contradictory conclusions on the occurrence of a dynamic transition in the same system. The IINS spectroscopy has proved to be very sensitive to the changes in the dynamics of hydrogen-containing functional groups in the polymorphs of glycine, having revealed a dynamic change at about 150 K that was not detected earlier by IR-spectroscopy,[29] calorimetry,[15,16] or X-ray diffraction[11] but manifests itself in the NMR spectra.[80] This change was interpreted as related to torsional vibrations of the NH_3 groups, similarly to the conclusions made previously for L-alanine.[52,77] Transitions at similar temperatures were reported for L-alanine,[77] for the model NMA (*N*-methylacetamide) system[92] and in the methyl groups of side chains polymers.[59,93]

In the crystalline amino acids with the side chains involved in hydrogen bonding, i.e., in L-serine (stronger H-bonds formed by the $-CH_2OH$) and in L-cysteine (weaker H-bonds formed by the $-CH_2SH$), the dynamic transitions corresponding to the reorientation of the side chains were observed at lower temperatures.[51,94,95] Interestingly enough, the dynamic transition involving the reorientation of the $-CH_2OH$ groups in L-serine manifests itself in the changes in the Raman[95] and IINS[51] spectra, whereas that of the $-CH_2SH$ residues in L-cysteine is clearly seen in the heat capacity temperature dependence,[94,96,5] in the variable-temperature IR,[97] and Raman[98] spectra and even in the X-ray structural data[94] but not in the $u^2(T)$ dependence measured by IINS.[99]

The dynamical transition observed in glycine, around 150−230 K, occurs at a very similar temperature as the common dynamic transitions in hydrated proteins[60,100,101] and transitions in some glass-forming systems.[102] In this respect, a detailed knowledge of the intermolecular potentials of amino acids in crystals and in the biopolymers is of crucial importance to discriminate between universal and specific features of proteins.

Acknowledgment. We acknowledge the support of the Berlin Neutron Scattering Center (BENSC) and the Institut Laue-Langevin in providing the neutron research facilities used in this work. H.N.B. thanks D.N. Argyriou for fruitful discussions. E.V.B. acknowledges the financial support of her stay at HMI and ILL and partial financial support of this work from RFBR (grant 05-03-32468) and from the SB RAS (Projects Nos. 49 and 110) as well as the assistance of Mr. A. F. Achkasov in preparing the samples of pure α- and γ-glycine and of Dr. T.N. Drebushchak in the characterization of these samples by X-ray powder diffraction. H.N.B. and E.V.B. would like to thank Jean-Luc Laborier and Louis Melezi for the skillful support during the pressure experiments at the ILL.

References and Notes

(1) Boldyreva, E. V. *In Models, Mysteries, and Magic of Molecules*; Boeyens, Jan C.A., Ogilvie, John F., Eds.; Springer: New York, 2008; pp 167−192.
(2) Bernal, J. D. *Z. Kristallogr.* **1931**, *78*, 363.
(3) McCammon, J. A.; Karplus, M. *Annu. Rev. Phys. Chem.* **1980**, *3*, 29.
(4) Karplus, M.; McCammon, J. A. *Annu. Rev. Biochem.* **1983**, *53*, 263.
(5) Kocis, T. J.; Cline, R. E.; Dlott, D. D. *J. Chem. Phys.* **1984**, *81*, 4932.
(6) Bridgman, P. W. *J. Biol. Chem.* **1914**, *19*, 511.
(7) Suresh, C. G.; Vijayan, M. *Int. J. Peptide Protein Res.* **1983**, *22*, 129.
(8) Marsh, R. E. *Acta Crystallogr.* **1958**, *11*, 654.
(9) Iitaka, Y. *Acta Crystallogr.* **1960**, *13*, 35.
(10) Iitaka, Y. *Acta Crystallogr.* **1961**, *14*, 1.
(11) Boldyreva, E. V.; Drebushchak, T. N.; Shutova, E. S. *Z. Kristallogr.* **2003**, *218*, 366.
(12) Boldyreva, E. V.; Ahsbahs, H.; Weber, H.-P. *Z. Kristallogr.* **2003**, *218*, 231.
(13) Boldyreva, E. V.; Drebushchak, V. A.; Drebushchak, T. N.; Paukov, I. E.; Kovalevskaya, Y. A.; Shutova, E. S. *J. Therm. Anal. Calorim.* **2003**, *73*, 409.
(14) Boldyreva, E. V.; Drebushchak, V. A.; Drebushchak, T. N.; Paukov, I. E.; Kovalevskaya, Y. A.; Shutova, E. S. *J. Therm. Anal. Calorim.* **2003**, *73*, 419.
(15) Boldyreva, E. V.; Drebushchak, V. A.; Kovalevskaya; Yu, A.; Paukov, I. E. *J. Therm. Anal. Calorim.* **2003**, *73*, 109.
(16) Drebushchak, V. A.; Boldyreva, E. V.; Kovalevskaya, Y. A.; Paukov, I. E.; Drebushchak, T. N. *J. Therm. Anal. Calorim.* **2005**, *79*, 65.
(17) Boldyreva, E. V.; Ivashevskaya, S. N.; Sowa, H.; Ahsbahs, H.; Weber, H.-P. *Dokl. Akad. Nauk* **2004**, 396–358.
(18) Murli, C.; Thomas, S.; Venkateswaran, S.; Sharma, S. M. *Physica B* **2005**, *364*, 233.
(19) Murli, C.; Sharma, S. M.; Karmakar, S.; Sikka, S. K. *Physica B* **2003**, *339*, 23.
(20) Goryainov, S. V.; Kolesnik, E. N.; Boldyreva, E. V. *Physica B* **2005**, *357*, 340.
(21) Boldyreva, E. V. *Cryst. Eng.* **2004**, *6*, 235.
(22) Boldyreva, E. V.; Ivashevskaya, S. N.; Sowa, H.; Ahsbahs, H.; Weber, H.-P. *Z. Kristallogr.* **2005**, *220*, 50.
(23) Goryainov, S. V.; Boldyreva, E. V.; Kolesnik, E. N. *Chem. Phys. Lett.* **2006**, *419*, 496.
(24) Dawson, A.; Allan, D. R.; Belmonte, S. A.; Clark, S. J.; David, W. I. F.; McGregor, P. A.; Parsons, S.; Pulham, C. R.; Sawyer, L. *Cryst. Growth Des.* **2005**, *5*, 1415.
(25) Drebushchak, T. N.; Boldyreva, E. V.; Shutova, E. S. *Acta Crystallogr.* **2002**, *58*, 634.
(26) Drebushchak, V. A.; Boldyreva, E. V.; Seryotkin,Yu, V.; Shutova, E. S. *J. Struct. Chem.* **2002**, *43*, 892.
(27) Tumanov, N. A.; Boldyreva, E. V.; Ahsbahs, H. *Powder Diffraction*, in press.
(28) Sakai, H.; Hosogai, H.; Kawakita, T.; Pnuma, K.; Tsukamoto, K. *J. Cryst. Growth* **1992**, *116*, 421.
(29) Chernobai, G. B.; Chesalov, Yu. A.; Burgina, E. B.; Drebushchak, T. N.; Boldyreva, E. V. *J. Struct. Chem.* **2007**, *48*, 322.
(30) Baran, J.; Ratajczak, H. *Vib. Spectrosc.* **2007**, *43*, 125.
(31) Baran, J.; Ratajczak, H. *Spectrochim. Acta* **2005**, *61A*, 1611.
(32) Tsuboi, M.; Onishi, T.; Nakagawa, I.; Shimanouchi, T.; Mizushima, S.-I. *Sprectrochim. Acta* **1958**, *12*, 253.
(33) Suzuki, S.; Shimanouchi, T. *Spectrochim. Acta* **1963**, *19*, 1195.
(34) Machida, K.; Kagayama, A.; Saito, Y.; Kuroda, Y.; Unoa, T. *Sprectrochim. Acta* **1977**, *33A*, 569.
(35) Husain, S. K.; Hasted, J. B.; Rosen, D.; Nicol, E.; Birch, J. R. *Infrared Phys.* **1984**, *24*, 201.
(36) Matei, A.; Drichko, N.; Gompf, B.; Dressel, M. *Chem. Phys.* **2005**, *316*, 61.
(37) Kettle, S. F. A.; Lugwisha, E.; Eckert, J.; McGuire, N. K. *Spectrochim. Acta* **1989**, *45A*, 533.
(38) Gorelik, V. S.; Zlobina, L. I.; Zubov, V. A. *J. Mol. Struct.* **1986**, *143*, 139.
(39) Shi, Y.; Wang, L. *J. Phys. D: Appl. Phys.* **2005**, *38*, 3741.
(40) See http://www.ncnr.nist.gov/resources/n-lengths/ for data on the neutron scattering cross-sections and scattering lengths.
(41) Hudson, B. S. *Vibration. Spectr.* **2006**, *42*, 25.
(42) Pawlukojc, A.; Leciejewicz, J.; Tomkinson, J.; Parker, S. F. *Spectrochim. Acta* **2002**, *58A*, 2897.
(43) Pawlukojc, A.; Leciejewicz, J.; Ramirez-Cuesta, A. J.; Nowicka-Scheibe, J. *Spectrochim. Acta* **2005**, *61A*, 2474.
(44) Pawlukojc, A.; Leciejewicz, J.; Natkaniec, I. *Spectrochim. Acta* **1996**, *52A*, 29.
(45) Pawlukojc, A.; Bajdor, K.; Dobrowolski, J. Cz.; Leciejewicz, J.; Natkaniec, I. *Spectrochim. Acta* **1997**, *A53*, 927.
(46) Pawlukojc, A.; Leciejewicz, J.; Tomkinson, J.; Parker, S. F. *Spectrochim. Acta* **2001**, *57A*, 2513.
(47) Thaper, C. L.; Dasannacharya, B. A.; Goyal, P. S.; Chakravarthy, R.; Tomkinson, J. *Physica B* **1991**, *174*, 251.
(48) Thaper, C. L.; Sinha, S. K.; Dasannacharya, B. A. Neutron scattering. In. *AIP Conf. Proc. No. 89* **1982**, 249.
(49) Powell, B. M.; Martel, P. *Chem. Phys. Lett.* **1979**, *67*, 165.
(50) Zhang, Y.; Zhang, P.; Ford, R. C.; Han, S.; Li, J. *J. Phys. Chem. B* **2005**, *109*, 17784.
(51) Bordallo, H. N.; Kolesov, B. A.; Boldyreva, E. V.; Juranyi, F. *J. Am. Chem. Soc.* **2007**, *129*, 10984.
(52) Barthes, M.; Vik, A. F.; Spire, A.; Bordallo, H. N.; Eckert, J. *J. Phys. Chem. A* **2002**, *106*, 5230.
(53) Glazkov, V. P.; Kozlenko, D. P.; Savenko, B. N.; Somenkov, V. A. *J. Exp. Theor. Phys.* **2000**, *90*, 319.
(54) Glazkov, V. P.; Kozlenko, D. P.; Savenko, B. N.; Somenkov, V. A.; Syrykh, G. F.; Telepnev, A. S. *J. Exp. Theor. Phys.* **2002**, *94*, 1134.

(55) Drebushchak, V. A.; Boldyreva, E. V.; Drebushchak, T. N.; Shutova, E. S. *J. Cryst. Growth* **2002**, *241*, 266.
(56) Lechner, R. E. *Physica B* **1992**, *973*, 180–181.
(57) Nipko, J.; Loong, C.-K.; Loewenhaupt, M.; Braden, M.; Reichardt, W.; Boatner, L. *Phys. Rev. B* **1997**, *56*, 11584.
(58) Sidorov, V. A.; Sadykov, R. A. *J. Phys.: Condens. Matter* **2005**, *17*, S3005.
(59) Djurado, D.; Combet, J.; Bée, M.; Rannou, P.; Dufour, B.; Pron, A.; Travers, J. P. *Phys. Rev. B* **2002**, *65*, 184202.
(60) Doster, W.; Cusak, S.; Petry, W. *Nature* **1989**, *337*, 754.
(61) Willis, B. T. M.; Pryor, A. W. In *Thermal Vibrations in Crystallography*; Cambridge University Press: Cambridge, 1975.
(62) Lowensy, S. W. In *Theory of Neutron Scattering from Condensed Matter*; Oxford University Press: Oxford, 1984.
(63) Bee, M.; Djurado, D.; Combet, J.; Gonzalez, M. A. *Chem. Phys.* **2002**, *277*, 211.
(64) Kitchin, S. J.; Tutoveanu, G.; Steele, M. R.; Porter, E. L.; Harris, K. D. M. *J. Phys. Chem. B* **2005**, *109*, 22808.
(65) Wang, C. H.; Storms, R. D. *J. Chem. Phys.* **1971**, *55* (10), 5110.
(66) Andrew, E. R.; Hinshaw, W. S.; Hutchins, M. G.; Sjoblom, R. O. I. *Mol. Phys.* **1976**, *31* (5), 1479.
(67) Vasanthi, R.; Sharma, S. M. *Chem. Phys.* **2006**, *331*, 77.
(68) Freire, P. T. C.; Melo, F. E. A.; Mendes Filho, J.; Lima, R. J. C.; Teixeira, A. M. R. *Vib. Spectrosc.* **2007**, *45* (2), 99.
(69) Janik, J. M.; Mikuli, E.; Migdak-Mikuli, A.; Rachwalska, M.; Stanek, T.; Janik, J. A.; Otnes, K.; Svare, I. *Phys. Scr.* **1983**, *28*, 569.
(70) Krawczyk, J.; Mayer, J.; Natkaniec, I.; Nowina Konopka, M.; Pawlukojc, A.; Steinsvoll, O.; Janik, J. A. *Physica B* **2005**, *362*, 27.
(71) Sourisseau, C.; Bee, M.; Dworkin, A.; Jobic, H. *J. Raman Spectrosc.* **2005**, *16*, 44.
(72) Bee, M.; Jobic, H.; Sourisseau, C. *J. Phys. C: Solid State Phys.* **1985**, *18*, 5771.
(73) Howard, J.; Robson, K.; Waddington, T. C. *J. Chem. Soc., Dalton Trans.* **1982**, *5*, 977.
(74) Migdal-Mikuli, A.; Holderna-Natkaniec, K.; Mikuli, E.; Hetmanczyk, L.; Natkaniec, I. *Chem. Phys.* **2007**, *335*, 187.
(75) Kromhout, R. A.; Moulton, W. G. *J. Chem. Phys.* **1955**, *23*, 1673.
(76) El-Eithan, F. Y.; Bates, A. R.; Gough, W.; Somerford, D. J. *J. Phys: Condens. Matter.* **1992**, 249.
(77) de Souza, J. M.; Freire, P. T.C.; Bordallo, H. N.; Argyriou, D. N. *J. Phys. Chem. B* **2007**, *111*, 5034.
(78) Taylor, R. E.; Chim, N.; Dybowski, C. *J. Mol. Struct.* **2006**, *794*, 133.
(79) Gu, Z.; Ebisawa, K.; McDermott, A. *Solid State Nucl. Magn. Res.* **1996**, *7*, 161.
(80) Drebushchak, I. V.; Kozlova, S. G.; Boldyreva, E. V.; Semenov, A. R. *J. Mol. Struct.*, **2008**, DOI: 10.1016/j.molstruc.2008.03.009.
(81) Ichikawa, M. *J. Mol. Struct.* **2000**, *552*, 63.
(82) Middendorf, H. D. *Annu. Rev. Biophys. Bioeng.* **1984**, *13*, 425.
(83) Rousseau, D. L.; Bauman, R. P.; Porto, S. P. S. *J. Raman Spectrosc.* **1981**, *10*, 255.
(84) Magazù, S.; Migliardo, F.; Mondelli, C.; Romeo, G. *Chem. Phys.* **2003**, *292*, 247.
(85) Vijay, A.; Sathyanarayana, D. N. *J. Phys. Chem.* **1992**, *96*, 10735.
(86) Fisher, G.; Cao, X.; Cox, N.; Francis, M. J. *Chem. Phys.* **2005**, 313.
(87) Bordallo, H. N.; Barthès, M.; Eckert, J. *Physica B* **1997**, *24*, 1243–1138.
(88) Gupta, V. D.; Singh, R. D. *Chem. Phys. Lett.* **1970**, *5*, 218.
(89) Hayward, R. L.; Middendorf, H. D.; Wanderlingh, U.; Smith, J. C. *J. Chem. Phys.* **1995**, *102*, 5525.
(90) Clarage, J. B.; Clarage, M. S.; Phillips, W. C.; Sweet, R. M.; Caspar, D. L. D. *Proteins: Struct., Funct., Genetics* **1992**, *12*, 145.
(91) Burda, K.; Kruk, J.; Borgstadt, R.; Stanek, J.; Strzalka, K.; Schmid, G. H.; Kruse, O. *FEBS Lett.* **2003**, *535*, 159.
(92) Bordallo, H. N.; Argyriou, D. N.; Barthès, M.; Kalceff, W.; Rols, S.; Herwig, K. W.; Fehr, C.; Juranyi, F.; Seydel, T. *J. Phys. Chem. B* **2007**, *111*, 7725.
(93) Frick, B.; Fetters, L. J. *Macromolecules* **1994**, *27*, 974.
(94) Paukov, I. E.; Kovalevskaya, Y. A.; Drebushchak, V. A.; Drebushchak, T. N.; Boldyreva, E. V. *J. Phys. Chem. B.* **2007**, *111*, 9186.
(95) Kolesov, B. A.; Boldyreva, E. V. *J. Phys. Chem. B* **2007**, *111*, 14387.
(96) Paukov, I. E.; Kovalevskaya, Y. A.; Boldyreva, E. V. *J. Therm. Anal. Calorim*, in press (DOI: 10.1007/s10973-007-8697-0).
(97) Minkov, V. S.; Chesalov,Yu. A.; Boldyreva, E. V. *J. Struct. Chem.* **2008**, accepted.
(98) Kolesov, B. A.; Boldyreva, E. V.; Minkov, V. S.; Drebushchak, T. N. *J. Phys. Chem. B*, submitted for publication.
(99) Bordallo, H. N.; Boldyreva, E. V.; Koza, M. Unpublished work.
(100) Magazu, S.; Maisano, G.; Migliardo, F.; Mondelli, C. *Biophys. J.* **2004**, *86*, 3241.
(101) Bizzarri, A. R. *J. Phys.: Condens. Matter* **2004**, *16*, 83.
(102) Frick, B.; Richter, D. *Science* **1995**, *267*, 1939.

JP8014723